COMMUNICATIONS IN COMPUTATIONAL PHYSICS
Vol. **4**, No. 5, pp. 1069-1085

Commun. Comput. Phys.
November 2008

A Multiple Temperature Kinetic Model and its Application to Near Continuum Flows†

Kun Xu* and Hongwei Liu

Mathematics Department, Hong Kong University of Science and Technology, Clear Water Bay, Kowloon, Hong Kong.

Received 26 February 2008; Accepted (in revised version) 28 May 2008

Available online 16 July 2008

Abstract. In an early approach, we proposed a kinetic model with multiple translational temperature [K. Xu, H. Liu and J. Jiang, Phys. Fluids **19**, 016101 (2007)]. Based on this model, the stress strain relationship in the Navier-Stokes (NS) equations is replaced by the translational temperature relaxation terms. The kinetic model has been successfully used in both continuum and near continuum flow computations. In this paper, we will further validate the multiple translational temperature kinetic model to flow problems in multiple dimensions. First, a generalized boundary condition incorporating the physics of Knudsen layer will be introduced into the model. Second, the direct particle collision with the wall will be considered as well for the further modification of particle collision time, subsequently a new effective viscosity coefficient will be defined. In order to apply the kinetic model to near continuum flow computations, the gas-kinetic scheme will be constructed. The first example is the pressure-driven Poiseuille flow at Knudsen number 0.1, where the anomalous phenomena between the results of the NS equations and the Direct Simulation Monte Carlo (DSMC) method will be resolved through the multiple temperature model. The so-called Burnett-order effects can be captured as well by algebraic temperature relaxation terms. Another test case is the force-driven Poiseuille flow at various Knudsen numbers. With the effective viscosity approach and the generalized second-order slip boundary condition, the Knudsen minimum can be accurately obtained. The current study indicates that it is useful to use multiple temperature concept to model the non-equilibrium state in near continuum flow limit. In the continuum flow regime, the multiple temperature model will automatically recover the single temperature NS equations due to the efficient energy exchange in different directions.

PACS: 47.10.ad, 47.11.-j, 47.11.St

Key words: Navier-Stokes equations, gas-kinetic model, non-equilibrium flows.

†Dedicated to Professor Xiantu He on the occasion of his 70th birthday.

*Corresponding author. *Email addresses:* makxu@ust.hk (K. Xu), hwliu@ust.hk (H. Liu)

1 Introduction

The transport phenomena, i.e., mass, heat, and momentum transfer, in different flow regime is of a great scientific and practical interest. The classification of various flow regimes is based on the dimensionless parameter, i.e., the Knudsen number, which is a measure of the degree of rarefaction of the medium. The Knudsen number Kn is defined as the ratio of the mean free path to a characteristic length scale of the system. In the continuum flow regime, i.e., $Kn < 0.001$, the Navier-Stokes equations with linear relations between stress and strain and the Fourier's law for heat conduction are adequate to model the fluid behavior. For flows in the continuum-transition regime ($0.1 < Kn < 1$), the Navier-Stokes equations are known to be inadequate. This regime is important for many practical engineering problems, such as the simulation of microscale flows [10] and hypersonic flow around space vehicles in low earth orbit [9]. Hence, there is a strong desire and requirement for accurate models which give reliable solutions with lower computational costs.

Currently, the DSMC method is the most successful technique in the numerical prediction of low density flows [3]. However, in the continuum-transition regime, especially for the micro-channel flows, the DSMC suffers from statistical noise in the bulk velocity because of the random molecular motion. When the bulk velocity is much slower than the thermal velocity, many independent samples are needed to eliminate the statistical scattering, as for the micro-electro-mechanical system (MEMS) simulation. Alternatively, many macroscopic continuum model have been intensively developed in the literature, which include the Burnett and super-Burnett equations [4, 18], Grad's 13 moment equations [5], the regularized 13 equations [14], and many others. For high-order equations, besides the difficulties in constructing the boundary condition, another assumption is that any non-equilibrium state is only a certain perturbation of the equilibrium one. In reality, the non-equilibrium state in the near continuum flow regime may not be able to be recovered from a simple truncated expansion of an equilibrium state.

In [21], based on the gas-kinetic Bhatnagar-Gross-Krook (BGK) equation, a kinetic model with multiple translational temperature for the continuum and near continuum flow simulation was proposed. In this approach, the energy exchanges among x-, y-, and z-directions are modeled through the particle collision. Based on the kinetic model, the viscous term in the Navier-Stokes equations is replaced by the temperature relaxation in the extended NS formulations. In the continuum flow regime, the standard Navier-Stokes solutions are precisely recovered. The numerical results presented in [21] are in good agreement with the DSMC data for a wide range of Kn numbers. The anomalous temperature minimum phenomena in the force-driven Poiseuille flow case at $Kn = 0.1$ between the Navier-Stokes solutions and the DSMC results are well captured by the multiple temperature kinetic model. The current study is to further develop the multiple temperature model by the following. First, in order to incorporate the flow physics near the wall, such as the flow behavior inside the Knudsen layer, the particle-particle collision as well as particle-wall collisions will be included in the current model through the modifi-

cation of the particle collision time (viscosity coefficient) [6]. Second, in order to improve the accuracy at boundary, a boundary condition based on the second-order derivatives of flow variables will be implemented. Many tests will be conducted for the near continuum flows. The first one is the pressure-driven Poiseuille flow at $Kn = 0.1$. The standard Navier-Stokes solutions present an opposite pressure curvature in the cross-stream direction in comparison with the DSMC solutions [20, 24]. Even though this anomalous phenomena can be resolved using the Burnett equations. However, with the use of multiple temperature the discrepancy can be much easily resolved using the current kinetic model. The second example is the force-driven Poiseuille flow at various Knudsen numbers. With the effective viscosity approach and the generalized second-order slip boundary condition, the well-known Knudsen's minimum can be captured. The third example is about the cavity flow in the transitional flow regime.

In this paper, Section 2 presents the kinetic multiple translational temperature model and the kinetic scheme to solve the new model. Section 3 is about the implementation of effective viscosity approach near the wall with the inclusion of both particle-particle and particle-wall collisions. At the same time, a generalized second-order slip boundary condition is presented. Numerical results are shown in Section 4. The last section is the conclusion.

2 Multiple translational temperature kinetic model and its numerical scheme

In this section, we briefly review the construction of the multi-temperature (multi-T) kinetic model for monatomic gas and the construction of the corresponding finite volume gas-kinetic scheme.

2.1 Multi-temperature gas-kinetic model

For non-equilibrium flow in the near continuum regime, one of the traditional approach is to derive the macroscopic governing equation based on the Boltzmann equation. In the process of deriving the macroscopic governing equations, the gas distribution function is usually approximated by an expansion around an equilibrium state, such as the Maxwellian distribution function. The main reason underlying this approach is that it has been proved that the Maxwellian is the only and unique one where the system will approach to eventually for an isolated system. However, for a non-equilibrium flow, the competition between the particle collisions to get to equilibrium and the particle transport to deviate away from the equilibrium, will make the gas stay in a non-equilibrium state forever. In this case, the purely mathematical expansion of a gas distribution around a Maxwellian may not be appropriate. A physical model with the consideration of specific non-equilibrium properties may become necessary. In the current study, we are going to adopt a two step approximation. In the first step, it will be assumed that the gas

distribution function will approach to a multiple translational temperature equilibrium state. Then, the multiple temperature equilibrium state relaxes to a equal temperature Maxwellian. The deviation between the multiple temperature "equilibrium" and the absolute Maxwellian depends on the local Knudsen number. The above multistage kinetic model corresponds to an extended Navier-Stokes equations, where the stress strain relationship will be replaced by the temperature relaxations. In the following, the detailed kinetic model will be presented.

This paper mainly concerns the 2-D flow simulation. In the following, the multiple temperature model in 2-D will be presented. The generalized BGK model can be derived from the original BGK model [2],

$$\begin{aligned}\frac{\partial f}{\partial t}+u\frac{\partial f}{\partial x}+v\frac{\partial f}{\partial y}&=\frac{f^{eq}-f}{\tau}\\&=\frac{g-f}{\tau}+\frac{f^{eq}-g}{\tau}\\&=\frac{g-f}{\tau}+Q,\end{aligned}\tag{2.1}$$

where the equilibrium state f^{eq} is the single temperature Maxwellian, and the multiple temperature state g has a general form

$$g=\frac{\rho}{(2\pi)^{3/2}}\frac{1}{|\epsilon|^{1/2}}\exp\Big(-\frac{1}{2}(u_i-U_i)_i\lambda_{ij}(u_j-U_j)\Big),$$

where $\epsilon=\lambda^{-1}$. The above distribution function has the similarity with Holway's ES-BGK model [8], but it comes from different physical consideration in the description of gas relaxation process. The detailed differences will be pointed out at the end of this subsection. In the current paper, we only consider a simple case, where the above temperature tensor is diagonal matrix and has the following form,

$$g=\rho\left(\frac{l_x}{\pi}\right)^{1/2}\left(\frac{l_y}{\pi}\right)^{1/2}\left(\frac{l_z}{\pi}\right)^{1/2}\exp\left[-l_x(u-U)^2-l_y(v-V)^2-l_zw^2\right].\tag{2.2}$$

Here $l_x=m/(2kT_x)$, $l_y=m/(2kT_y)$, and $l_z=m/(2kT_z)$ are related to the translational temperature T_x, T_y, and T_z in $x-$, $y-$ and $z-$directions. In order to determine all unknowns in the corresponding macroscopic variables, such as ρ, U, V, T_x, T_y, and T_z, we propose the following moments for the collision term in the BGK model,

$$\begin{aligned}&\int\phi\left(\frac{\partial f}{\partial t}+u\frac{\partial f}{\partial x}+v\frac{\partial f}{\partial y}\right)dudvdw\\&=\int\phi\Big(\frac{g-f}{\tau}+Q\Big)dudvdw=\Big(0,0,0,0,(\rho E_x^{eq}-\rho E_x)/\tau,(\rho E_y^{eq}-\rho E_y)/\tau\Big)^T,\end{aligned}\tag{2.3}$$

where

$$\phi=\left[1,u,v,\frac{1}{2}(u^2+v^2+w^2),\frac{1}{2}u^2,\frac{1}{2}v^2\right]^T.$$

The first four moments on the right hand side of Eq. (2.3) are the conservative moments of the mass, momentum, and total energy. The last two moments are related to the energy exchange among different directions. The equilibrium energies ρE_x^{eq} and ρE_y^{eq} in Eq. (2.3) have the forms

$$\rho E_x^{eq} = \frac{1}{2}\rho U^2 + \frac{\rho}{4l^{eq}}$$

and

$$\rho E_y^{eq} = \frac{1}{2}\rho V^2 + \frac{\rho}{4l^{eq}},$$

which are constructed based on the assumption that the system will approach to an equal temperature equilibrium state. The single equilibrium temperature l^{eq} is determined by equally distributing thermal energy in all directions,

$$\rho\frac{3}{4l^{eq}} = \rho E - \frac{1}{2}\rho(U^2+V^2),$$

where ρE is the total energy, i.e.,

$$\rho E = \int \frac{1}{2}(u^2+v^2+w^2) f du dv dw = \int \frac{1}{2}(u^2+v^2+w^2) g du dv dw.$$

The tendency for the gas distribution function to approach to a common Maxwellian determined by $(\rho, U, V, \lambda^{eq})$ means that the H-theorem for the system (2.1) and (2.3) is satisfied. Note that the last two moments on the right hand side of Eq. (2.3) is due to the term Q in the collision term of the BGK equation (2.1). Therefore, there is no source term contribution for the term $(g-f)/\tau$, and this property is precisely used in the development of the numerical scheme. The numerical scheme based on Eqs. (2.1) and (2.3) for the time evolution of macroscopic physical quantities will be presented later. The physical idea in our kinetic model is that the thermal equilibrium between x-, y-, and z-directions will be achieved through the particle collisions, and there is a time delay to achieve the temperature equilibrium. However, in the Navier-Stokes equations, it is assumed that the same equilibrium temperature is obtained instantaneously. The Navier-Stokes assumption between the stress and the velocity gradient is only valid in the continuum flow limit. The real viscosity terms in the NS equations are replaced by the temperature relaxation term from the current model.

Remark 2.1. Even though there is similarity between the mid-equilibrium state g in the current model and Holway's ES-BGK model [8], the physical consideration is different. In the ES-BGK model, the only collision process is from f to g and this collision term cannot generate the compatibility condition in Eq. (2.3), where the non-zero terms are solely from the non-conservative process from g to f^{eq}.

Remark 2.2. In this paper, the original BGK collision term is divided into two subprocesses. For a nonlinear gas system, this division, even zero-added mathematically, will be different physically due to different gas evolution path. Also, the current model

has advantages when handling diatomic gas, where the relaxation times for different physical processes, such as rotational equilibrium, may be different.

Remark 2.3. The current model explicitly presents the different temperature concept and considers it as a physical reality. In Holway's ES-BGK model, a single translational temperature is actually used. The stress tensor and a free parameter are introduced into the ellipsoid distribution function in order to fix the Prandtl number in its Chapman-Enskog expansion up to the Navier-Stokes order. For a gas with unit Prandtl number, the ES-BGK model will shrink to the original BGK model exactly. However, for the current multiple translational temperature model, even with unit Prandtl number, different temperatures are still there. Based on the Chapman-Enskog expansion, the ES-BGK model basically recovers the Navier-Stokes equations [8] with a variable Prandtl number. To the same order in the Chapman-Enskog expansion, the current model will generate a much enlarged system and there are individual governing equation for each temperature in different direction.

Remark 2.4. In the current paper, only three temperatures are introduced to model the non-equilibrium flow properties in the near continuum regime. Theoretically, the real temperature should be a three-by-three symmetric tensor and there are six independent components.

2.2 Finite volume scheme for multi-T kinetic model

The kinetic model constructed in the previous subsection is solved based on the gas-kinetic BGK scheme [17]. It is a conservative multi-scale finite volume method, where the update of the macroscopic flow variables is through the numerical fluxes, which are evaluated based on the time-dependent gas distribution function at cell interfaces. Since we use a directional splitting method to solve Eq. (2.1), the kinetic model in x-direction can be written as,

$$f_t + u f_x = (g-f)/\tau + Q,$$

where g is the multiple temperature equilibrium state (2.2). Taking moments ϕ to the above equation in a control volume $x \in [x_{j-1/2}, x_{j+1/2}]$ and time interval $t \in [t^n, t^{n+1}]$, the update of the macroscopic flow variables, i.e., $\mathbf{W} = (\rho, \rho U, \rho V, \rho E, \rho E_x, \rho E_y)^T$ inside each numerical cell $[x_{j-1/2}, x_{j+1/2}]$ from time step t^n to t^{n+1}, becomes

$$\mathbf{W}_j^{n+1} = \mathbf{W}_j^n + \frac{1}{\Delta x}\int_{t^n}^{t^{n+1}} (\mathbf{F}_{j-1/2}(t) - \mathbf{F}_{j+1/2}(t))dt + \mathbf{S}_j^n \Delta t, \tag{2.4}$$

where $\mathbf{F}_{j+1/2}$ is the corresponding fluxes at a cell interface, which can be evaluated based on the gas distribution function $f_{j+1/2}$ there,

$$\mathbf{F} = \int u\phi f_{j+1/2} du dv dw.$$

The source term is due to the moments of the collision term in Eq. (2.3) which has the form

$$\mathbf{S}=(0,0,0,0,(\rho E_x^{eq}-\rho E_x)/\tau,(\rho E_y^{eq}-\rho E_y)/\tau)^T.$$

For the current multi-T model, the evaluation of the gas distribution function f at a cell interface is similar to the BGK-NS method in [17], where the only difference between them is that three temperatures T_x, T_y, and T_z have to be accounted for, see [21] for more details. After the determination of f at a cell interface, we can explicitly evaluate the heat flux there as well. In order to simulate the flow with any realistic Prandtl number, a modification of the heat flux in the energy transport, such as that used in [17], is also implemented in the present study. Therefore, the current model can simulate flow with any Prandtl number.

3 Effective viscosity coefficient and the generalized second-order slip boundary condition

It is well known that the physical significance of the viscosity is its effect on the momentum exchange between the fluid molecules. From kinetic theory, the viscosity coefficient μ is related to the mean free path l of gas molecules, such as $\mu=\delta\bar{c}\rho l$, where $\bar{c}$ is the mean molecular speed, ρ is the gas density and δ is taken to be a constant with a value of 0.499 [4]. In the near-wall region, however, the presence of a solid boundary will have a significant impact on the average distance a gas molecule can travel between successive collisions with either another gas molecule or the solid wall. To enable the Navier-Stokes equations to capture the velocity profile in the Knudsen layer, the construction of *effective viscosity* has been investigated in [11,22]. Here we use the method recently proposed by Guo *et al.* [6]. Let us consider a gas bounded by two parallel walls located at $z=0$ and $z=H$, respectively. The effective viscosity μ_e is defined by [6]

$$\mu_e(z)=\mu_0\left[1+\frac{1}{2}\Big((\alpha-1)e^{-\alpha}+(\beta-1)e^{-\beta}-\alpha^2E_i(\alpha)-\beta^2E_i(\beta)\Big)\right], \tag{3.1}$$

where $\alpha=z/l_0$ and $\beta=(H-z)/l_0$, and $E_i(x)$ is the exponential integral function given by

$$E_i(x)=\int_1^\infty t^{-1}e^{-xt}dt. \tag{3.2}$$

The generalized second-order slip boundary condition is also adopted in our numerical simulation:

$$u|_s-u|_w=\left(l(\frac{\partial u}{\partial z})-\frac{1}{2}l\frac{\partial}{\partial z}(l\frac{\partial u}{\partial z})\right)_w \tag{3.3}$$

with $l=l_0\mu/\mu_0$. The validity of the above effective viscosity method as well as the generalized slip boundary condition has been presented in [6].

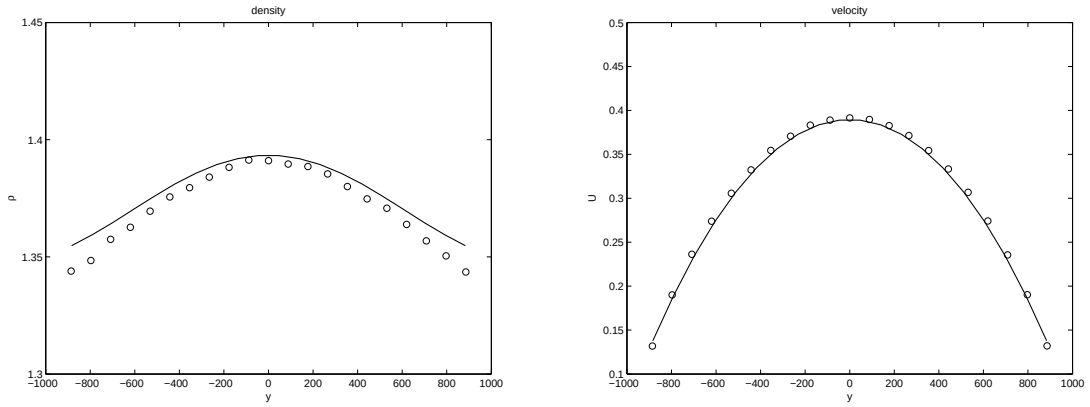

Figure 1: Nondimensional density (left) and velocity (right) profiles in the cross-stream direction at $x=0$, solid line is multi-T model solution and circle is DSMC data [24].

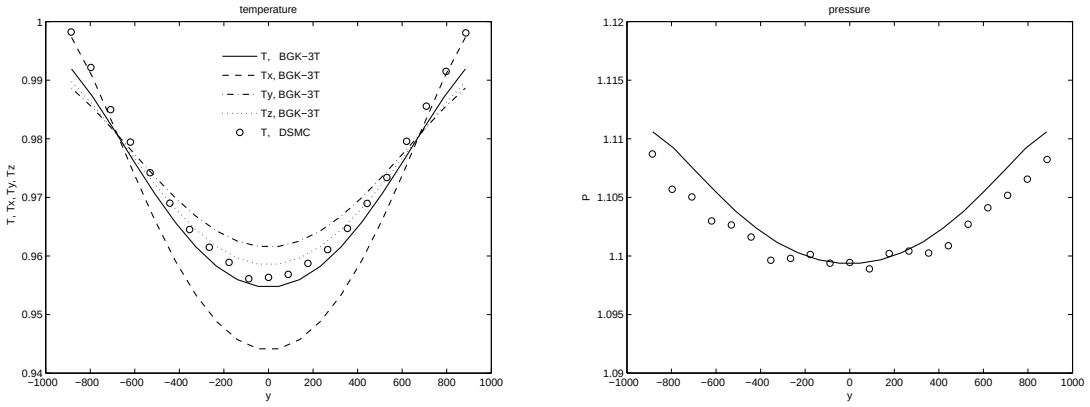

Figure 2: Nondimensional temperature (left) and pressure (right) profiles in the cross-stream direction at $x=0$, solid line is multi-T model solution and circle is DSMC data [24]. The averaged temperature T on the left figure is defined by $T=(T_x+T_y+T_z)/3$.

4 Numerical experiments

4.1 Pressure-driven Poiseuille flows at $Kn=0.1$

It is generally recognized that in the slip flow regime with Knudsen number Kn≤ 0.1, the Navier-Stokes equations with the slip boundary condition is capable to accurately simulate the microchannel flow. However, for the simple force-driven and pressure-driven Poiseuille flows in the slip flow regime with relative small gradients and Knudsen number, the Navier-Stokes equations give qualitatively incorrect predictions [23, 24]. In the force-driven case, they fail to reproduce the central minimum in the temperature profile and non constant pressure profile, which are both predicted by the kinetic theory and observed in the DSMC simulation [1, 7, 12, 15, 16]. In the pressure-driven case, the pres-

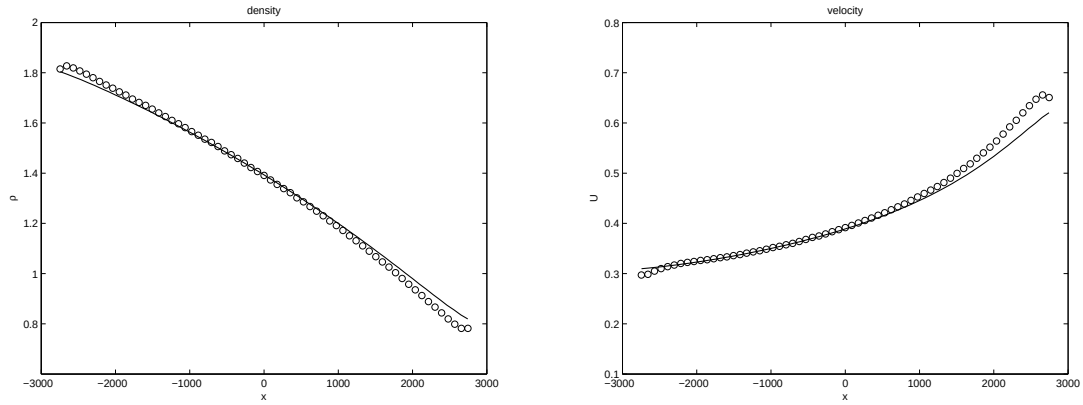

Figure 3: Nondimensional density (left) and velocity (right) profiles in the stream-wise direction at $y=0$, solid line is multi-T model solution and circle is DSMC data [24].

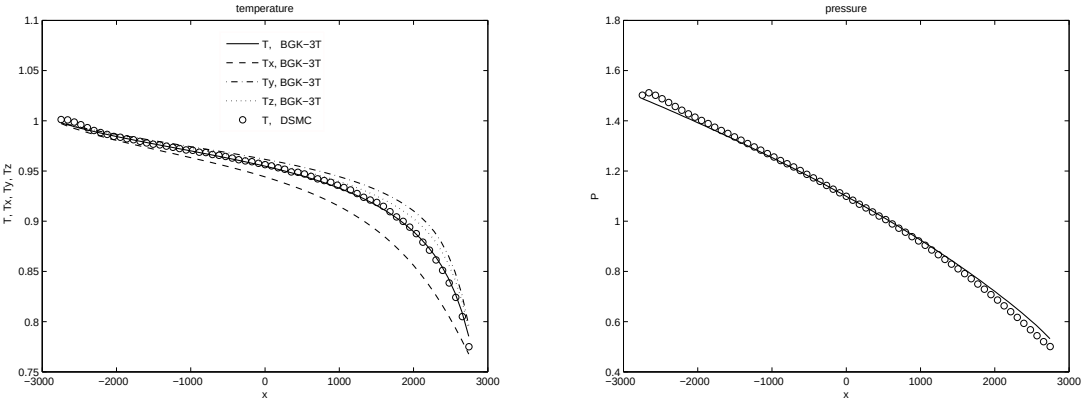

Figure 4: Nondimensional temperature (left) and pressure (right) profiles in the stream-wise direction at $y=0$, solid line is multi-T model solution and circle is DSMC data [24]. The averaged temperature T on the left figure is defined by $T=(T_x+T_y+T_z)/3$.

sure profiles in the cross-stream direction from the Navier-Stokes solutions and DSMC data have the opposite curvature [20, 24]. Furthermore, it is not possible to correct this failure by modifying the equation of state, transport coefficients or boundary conditions, and the discrepancy is solely caused by the governing equations themselves. In order to understand these phenomena, many analysis have been done. For example, the non-constant pressure is well explained based on the Burnett equations [16], and the temperature minimum at the center is explained only through the kinetic theory [1, 7, 12, 15], or the super-Burnett solution [18]. As an excellent test for capturing non-equilibrium phenomena, the current multi-temperature model will be used to study the pressure-driven Poiseuille flows at $Kn=0.1$.

The set up of the Poiseuille flows is given in [23]. The simulation fluid is a hard sphere gas with particle mass m=1 and diameter d=1. At the reference density of ρ_0=1.21×10^{-3},

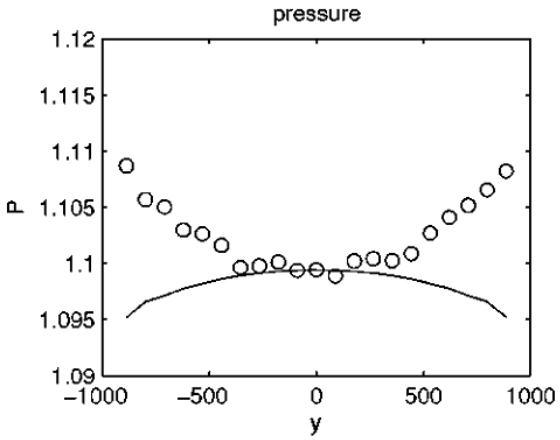

Figure 5: Nondimensional pressure profile in the cross-stream direction at $x=0$, solid line is BGK-NS solution and circle is DSMC data [24].

the mean free path is $l_0=m/(\sqrt{2}\pi\rho_0 d^2)=186$. The distance between the thermal walls is $L_y=10l_0$ and their temperature is $T_0=1$. The reference fluid speed is $U_0=\sqrt{2kT_0/m}=1$, so Boltzmann constant is taken as $k=1/2$. The reference sound speed is $c_0=\sqrt{\gamma kT_0/m}=0.91$ with $\gamma=5/3$ for a monatomic gas. The reference pressure is $p_0=\rho_0 kT_0/m=6.05\times10^{-4}$. For the pressure-driven case, $dp/dx\approx1.08\times10^{-7}$ with $p_{in}=\frac{3}{2}p_0$, $p_{out}=\frac{1}{2}p_0$ and $L_x=3L_y=30l_0$. In these cases the Knudsen number is $Kn=l_0/L_y=0.1$ and the Reynolds number is of order one. In all calculations, the cell size takes the size of one fifth of the mean free path under the initial flow condition. Maxwell diffusive kinetic boundary condition [20] with the accommodation coefficient $\sigma=1$ is used.

The results for the pressure-driven case from the multi-T kinetic model are shown in Figs. 1-2 and 3-4. Although the Navier-Stokes equations give opposite-curvature pressure profile in comparison with the DSMC data, see Fig. 5, the agreement between the results from the multi-T kinetic model and the DSMC method is quite good (Fig. 2, right), which shows the multi-T model has the advantage over the Navier-Stokes equations in capturing the non-equilibrium physical phenomena in the near continuum flow regime. The distributions of flow variables along the stream-wise direction also agree well with DSMC results which are shown in Figs. 3-4.

4.2 Force-driven Poiseuille flow at various Knudsen numbers

The force-driven Poiseuille flow at different Knudsen numbers is calculated using the multi-T kinetic model as well. The accurate analysis of the problem has been carried out by many authors [10]. One of the benchmark results is the solution of the Boltzmann equation, which has been obtained by Ohwada *et al.* [13] for hard-sphere (HS) molecules. In our computation, the working gas is argon with molecular mass $m=6.63\times10^{-26}$ kg. The dynamical viscosity coefficient for HS gas is $\mu=2.117\times10^{-5}\sqrt{T/273}\mathrm{Ns/m^2}$. The

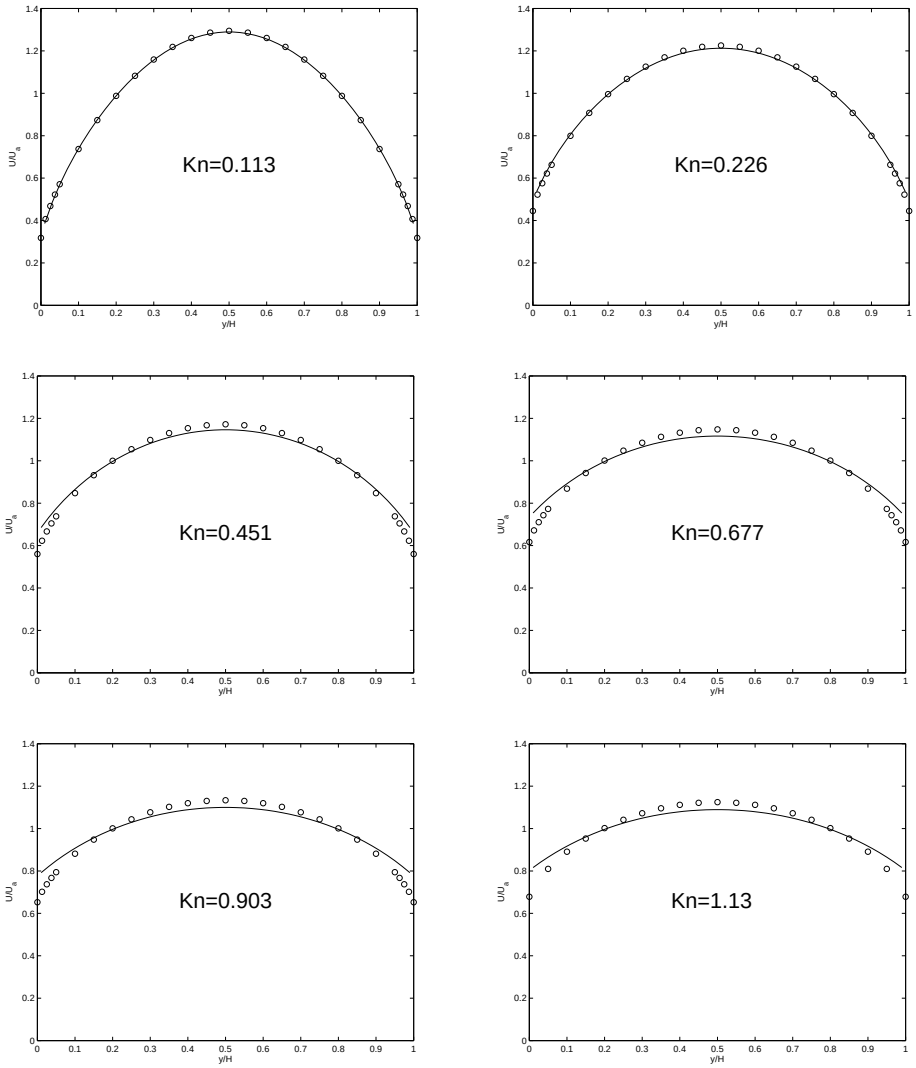

Figure 6: Nondimensional velocity profiles for force-driven Poiseuille flow at Knudsen numbers of 0.113, 0.226, 0.451, 0.677, 0.903, and 1.13. Circle is the solution of the linearized Boltzmann equation by Ohwada *et al.* [13], and solid line is from the multi-T kinetic model.

mean free path is defined by

$$l_0 = \frac{16}{5}\left(\frac{1}{2\pi RT}\right)^{1/2}\frac{\mu}{\rho_0}, \tag{4.1}$$

where R is the gas constant, and T and ρ_0 are temperature and density, respectively. The density ρ_0 has a value corresponding to the pressure of 1 atm and $T = 273$K. The accommodation coefficient is taken as $\sigma = 1$ for both walls, and the effective viscosity and the generalized slip boundary condition are employed in our numerical simulation.

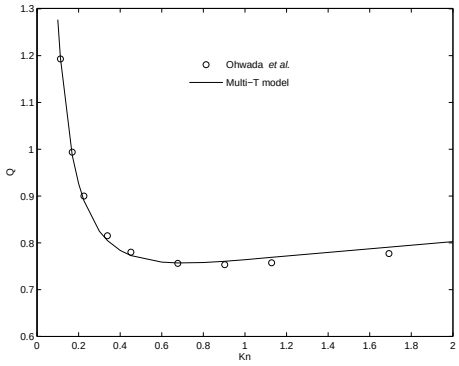

Figure 7: Nondimensional flow rate Q as a function of the Knudsen number for force-driven Poiseuille flow. Circle is the solution of the linearized Boltzmann equation by Ohwada *et al.* [13], and solid line is from the multi-T kinetic model.

The velocity distributions for both the linearized Boltzmann equation by Ohwada *et al.* [13] and the multi-T kinetic model at different Knudsen numbers are shown in Fig. 6. For this problem, the nondimensional velocity is defined as U/U_a, where U_a is the mean velocity across the channel. As expected, the discrepancy between our predictions and the solution of the linearized Boltzmann equation increases with the Knudsen number. However, our numerical results are comparable with those using the wall-function approach in [22], which has significant improvement over the conventional Navier-Stokes slip-flow solution. The normalized mass flow rate is shown in Fig. 7, from which we can see that the well-known Knudsen's minimum is well captured by the kinetic model.

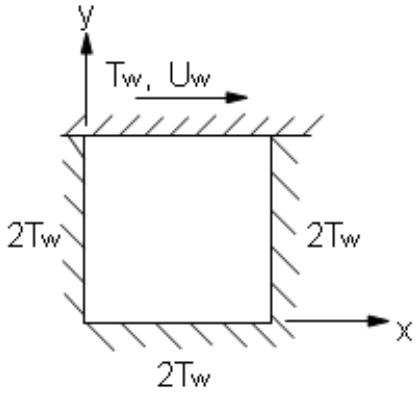

Figure 8: Cavity flow.

4.3 2D cavity flow at $Kn = 0.1$

The 2D cavity flow will be simulated here. Fig. 8 shows the schematic graph for this case, where the upper wall keeps the temperature $T_w = 273K$ and moves to the right

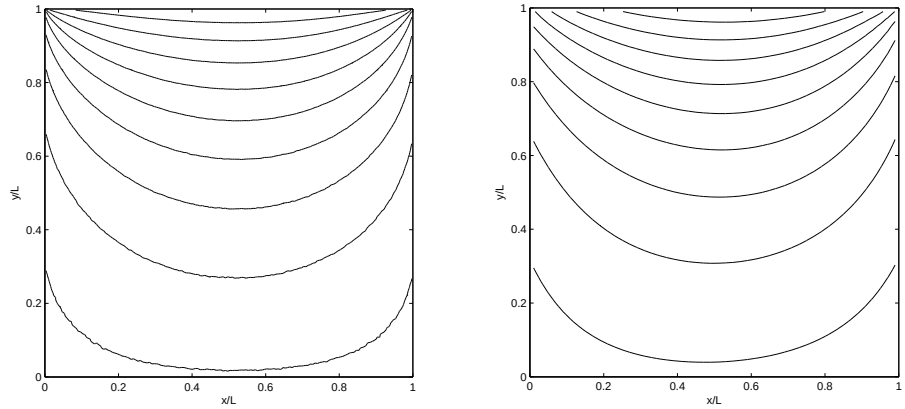

Figure 9: Contours of the averaged temperature T, i.e. $T=(T_x+T_y+T_z)/3$, by DSMC (left) and the current multi-T model (right). In both figures, 9 equally spaced contours from $T=350K$ to $T=530K$ are plotted.

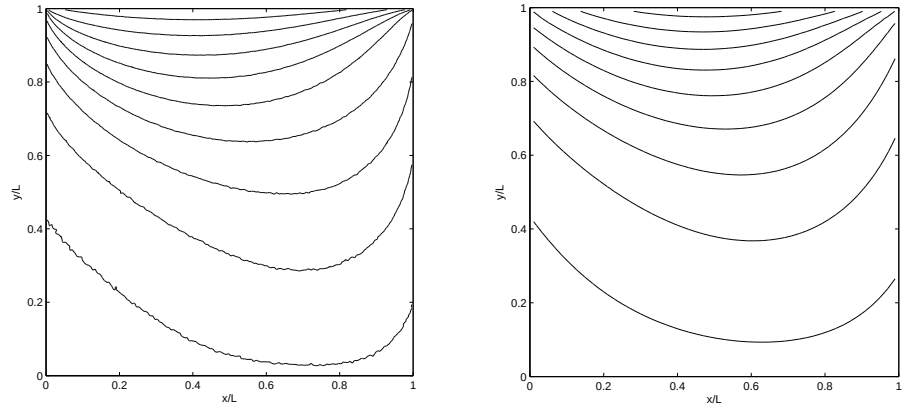

Figure 10: Contours of the temperature T_x by DSMC (left) and the current multi-T model (right). In both figures, 9 equally spaced contours from $T_x=350K$ to $T_x=530K$ are plotted.

along positive x direction with the velocity U_w, and other three stationary walls keep the temperature $2T_w=2\times 273K$. The working gas is argon with the dynamical viscosity coefficient

$$\mu=2.117\times 10^{-5}\left(\frac{T}{T_w}\right)^{\omega}, \tag{4.2}$$

where $\omega=0.81$. Initially, the gas is static with temperature T_w and pressure $1atm$ (or $101325Pa$), and the density can be obtained from the equation of state for perfect gas $p=\rho RT$, where R is the gas constant defined by $R=k/m$ with Boltzmann constant k and molecular mass m. The numerical results are compared with DSMC solutions from the variable hard sphere (VHS) model. For this model, the mean free path of the gas is

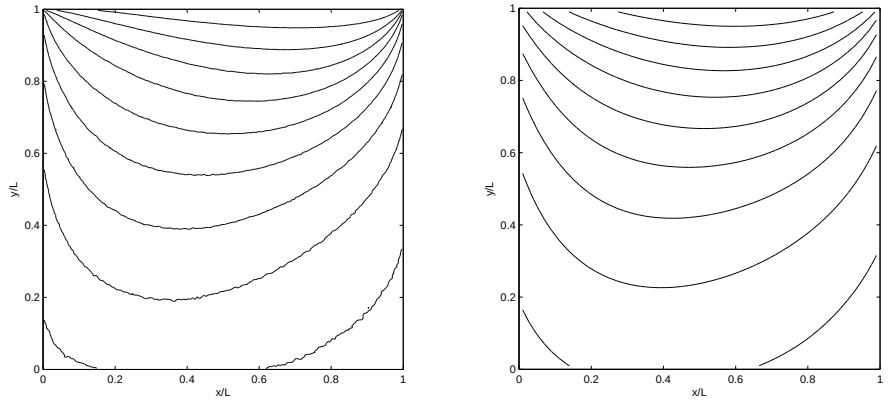

Figure 11: Contours of the temperature T_y by DSMC (left) and the current multi-T model (right). In both figures, 9 equally spaced contours from $T_y=350K$ to $T_y=530K$ are plotted.

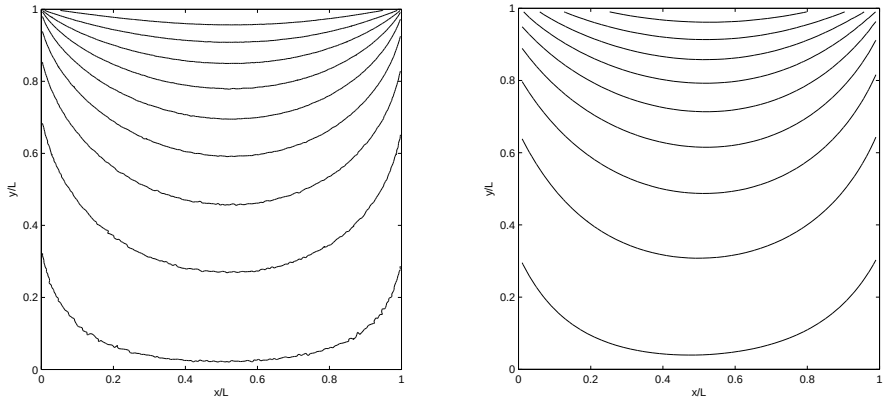

Figure 12: Contours of the temperature T_z by DSMC (left) and the current multi-T model (right). In both figures, 9 equally spaced contours from $T_z=350K$ to $T_z=530K$ are plotted.

defined by

$$\lambda=\frac{4(7-2\omega)(5-2\omega)}{30\sqrt{\pi}}\times\frac{\mu}{\rho c}, \tag{4.3}$$

where c is the most probable speed $c=\sqrt{2RT}$. From the initial condition, we can get the corresponding mean free path $\lambda_0=4.82\times10^{-8}m$, then the side length of cavity is determined by $L=\lambda_0/Kn$ with a given Knudsen number Kn. Here we let $Kn=0.1$. The velocity U_w of the upper moving wall is chosen so that the corresponding Mach number $M_a=U_w/\sqrt{\gamma RT_w}$ takes the value of 0.3 with $\gamma=5/3$.

The numerical results from both the current multi-T kinetic model and the DSMC are shown in Figs. 9-12. These temperature contours show good agreement between the multi-T model and DSMC solutions. In these cases, the different temperature (T_x,T_y,T_z) distributions are clearly observed, especially for the temperature T_x and T_y.

5 Conclusion

The kinetic model with multiple translational temperature [21] was applied for some near continuum flow simulation. In the pressure-driven Poiseuille flow at $Kn = 0.1$, the Navier-Stokes equations and the DSMC results present pressure profiles with opposite curvature in the cross-stream direction. The multi-T kinetic model gives results which agree well with the DSMC data. For the force-driven Poiseuille flow at various Knudsen numbers, with the effective viscosity approach and the generalized second-order slip boundary condition [6], the well-known Knudsen's minimum is captured by the current model. Our numerical results indicate that the multiple temperature kinetic model and its numerical method provide a useful tool for the study of micro-flows in the near continuum flow regime.

The success of the current approach is mainly due to the following fact. Instead of expanding the gas distribution function around a local Maxwellian distribution function, such as the common approach used in the Chapman-Enskog expansion, we separate this process into two steps. First, the expansion is around a state g with multiple translational temperature. Then, this state will approach to a traditional equal-temperature equilibrium one f^{eq}. The distance between these two states depends on the Knudsen number. For a sustained non-equilibrium gas system in the near continuum flow regime, these two states will never approach to each other and the multiple temperature effect will become an important physical reality, such as the examples presented in this paper. In the continuum flow regime, due to the closeness of these two states, the traditional Navier-Stokes equations can be exactly recovered. The two steps approach may be useful also to modify the well-developed Chapman-Enskog expansion and moment methods to get the approximate solutions of the Boltzmann equation.

In the current paper, three individual temperatures in $x-$, $y-$, and $z-$direction for the middle state g are used in the kinetic model. If g is replaced by a general Gaussian distribution function with temperature as a symmetric tensor T_{ij}, a generalized Navier-Stokes system can be derived. In the non-equilibrium flow regime, the temperature T_{ij} represents the randomness of the particle motion which depends on the spatial orientation. The corresponding gas dynamic equations for this model have the same structure as the Navier-Stokes equations, but the NS constitutive relationship,

$$\sigma_{ij} = -p\delta_{ij} + \mu(\partial_i U_j + \partial_j U_i - \frac{2}{3}\partial_k U_k \delta_{ij})$$

is replaced by temperature relaxation terms

$$\sigma_{ij} = -\rho R T_{ij} + \rho R(T^{eq}\delta_{ij} - T_{ij}).$$

Also, in order to extend the current multiple translational temperature model to diatomic gas [19], more temperature components, i.e., six translational, one rotational, and multiple vibrational ones, have to be included.

Acknowledgments

The author would like to thank Dr. Jianzheng Jiang to provide the DSMC solution for the cavity flow test and Dr. Zhaoli Guo for helpful discussion. This research was supported by Hong Kong Research Grant Council 621005 and 621406.

References

[1] K. Aoki, S. Takata, and T. Nakanishi, *Poiseuille-type flow of a rarefied gas between two parallel plates driven by a uniform external force*, *Phys. Rev. E* **65**, 026315 (2002).
[2] P. L. Bhatnagar, E. P. Gross, and M. Krook, *A model for collision processes in gases. I: Small amplitude processes in charged and neutral one-component systems*, *Phys. Rev.* **94**, 511–525 (1954).
[3] G. Bird, *Molecular gas dynamics and the direct simulation of gas flows* (Clarendon Press, Oxford, 1994).
[4] S. Chapman and T. G. Cowling, *The Mathematical Theory of Non-Uniform Gases* (Cambridge University Press, Cambridge, 1971).
[5] H. Grad, *On the kinetic theory of rarefied gases*, *Commun. Pure Appl. Math.* **2**, pp. 325 (1949).
[6] Z.L. Guo, B.C. Shi. and C.G. Zheng, *An extended Navier-Stokes formulation for gas flows in the Knudsen layer near a wall* , *Europen Phys. Letter*, **80**, No. 2, 24001 (2007).
[7] S. Hess and M. Malek-Mansour, *Temperature profile of a dilute gas undergoing a plane Poiseuille flow*, *Physica A* **272**, 481-496 (1999).
[8] L.H. Holway, *New statistical models for kinetic theory: methods of construction*, *Physics of fluids* **9** (1966), pp. 1658-1673.
[9] M.S. Ivanov and S.F. Gimelshein, *Computational hypersonic rarefied flows*, *Annu. Rev. Fluid Mech.* **30**, 469-505 (1998).
[10] G. E. Karniadakis, A. Beskok and N. R. Aluru, *Microflows and Nanoflows: Fundamentals and Simulation* (Springer Press, New York, 2005).
[11] D. A. Lockerby, J. M. Reese and M. A. Gallis, *The usefulness of higher-order constitutive relations for describing the Knudsen layer*, *Phys. Fluids* **17**, 100609 (2005).
[12] M.M. Malek, F. Baras, and A.L. Garcia, *On the validity of hydrodynamics in plane Poiseuille flows*, *Physica A* **240**, 255-267 (1997).
[13] T. Ohwada, Y. Sone and K. Aoki, *Numerical analysis of the Poiseuille and thermal transpiration flows between two parallel plates on the basis of the Boltzmann equation for hard-sphere molecules*, *Phys. Fluids A* **1**(12), 2042-2049 (1989).
[14] H. Struchtrup and M. Torrilhon, *Regularization of Grad's 13 moment equations: derivation and linear analysis*, *Physics of Fluids* **15** (2003), pp. 2668-2680.
[15] M. Tij and A. Santos, *Perturbation analysis of a stationary non-equilibrium flow generated by an external force*, *J. Stat. Phys.* **76**, 1399-1414 (1994).
[16] F.J. Uribe and A.L. Garcia, *Burnett description for plane Poiseuille flow*, *Physical Review E* **60**, 4063-4078 (1999).
[17] K. Xu, *A gas-kinetic BGK scheme for the Navier-Stokes equations and its connection with artificial dissipation and Godunov method*, *J. Comput. Phys.* **171**, 289–335 (2001).
[18] K. Xu, *Super-Burnett solutions for Poiseuille flow*, *Phys. Fluids* **15**, No. 7, 2077-2080 (2003).
[19] K. Xu and E. Josyula, *Continuum formulation for non-equilibrium shock structure calculation*, *Communications in Computational Physics*, **1**, No. 3, pp. 425-450 (2006).

[20] K. Xu and Z.H. Li, *Microchannel flows in slip flow regime: BGK-Burnett solutions*, *J. Fluid Mechanics* **513**, 87-110 (2004).
[21] K. Xu, H. Liu and J. Jiang, *Multiple temperature kinetic model for continuum and near continuum flows*, *Phys. Fluids* **19**, 016101 (2007).
[22] Y. H. Zhang, X. J. Gu, R. W. Barber and D. R. Emerson, *Capturing Knudsen layer phenomena using a lattice Boltzmann model*, *Phys. Rev. E* **74**, 046704 (2006).
[23] Y. Zheng, A.L. Garcia, and B.J. Alder, *Comparison of kinetic theory and hydrodynamics for Poiseuille flow*, *Rarefied Gas Dynamics* 23, Whistler, Canada (2002).
[24] Y. Zheng, A.L. Garcia, and B.J. Alder, *Comparison of kinetic theory and hydrodynamics for Poiseuille flow*, *J. Statistical Phys.* **109**, 495-505 (2002).